NANO LETTERS

Letter

pubs.acs.org/NanoLett

Ultrafast Characterization of Phase-Change Material Crystallization Properties in the Melt-Quenched Amorphous Phase

Rakesh Jeyasingh,*[,†,¶] Scott W. Fong,[†] Jaeho Lee,[‡] Zijian Li,[‡] Kuo-Wei Chang,[§] Davide Mantegazza,[§] Mehdi Asheghi,[‡] Kenneth E. Goodson,[‡] and H.-S. Philip Wong[†]

[†]Department of Electrical Engineering, Stanford University, Stanford, California 94305, United States

[‡]Department of Mechanical Engineering, Stanford University, Stanford, California 94305, United States

[§]Intel Corporation, 2200 Mission College Blvd, Santa Clara, California 95054, United States

Supporting Information

ABSTRACT: Phase change materials are widely considered for application in nonvolatile memories because of their ability to achieve phase transformation in the nanosecond time scale. However, the knowledge of fast crystallization dynamics in these materials is limited because of the lack of fast and accurate temperature control methods. In this work, we have developed an experimental methodology that enables ultrafast characterization of phase-change dynamics on a more technologically relevant melt-quenched amorphous phase using practical device structures. We have extracted the crystallization growth velocity (U) in a functional capped phase change memory (PCM) device over 8 orders of magnitude ($10^{-10} < U < 10^{-1}$ m/s) spanning a wide temperature range ($415 < T < 580$ K). We also observed direct evidence of non-Arrhenius crystallization behavior in programmed PCM devices at very high heating rates (>10^8 K/s), which reveals the extreme fragility of $Ge_2Sb_2Te_5$ in its supercooled liquid phase. Furthermore, these crystallization properties were studied as a function of device programming cycles, and the results show degradation in the cell retention properties due to elemental segregation. The above experiments are enabled by the use of an on-chip fast heater and thermometer called as microthermal stage (MTS) integrated with a vertical phase change memory (PCM) cell. The temperature at the PCM layer can be controlled up to 600 K using MTS and with a thermal time constant of 800 ns, leading to heating rates ~10^8 K/s that are close to the typical device operating conditions during PCM programming. The MTS allows us to independently control the electrical and thermal aspects of phase transformation (inseparable in a conventional PCM cell) and extract the temperature dependence of key material properties in real PCM devices.

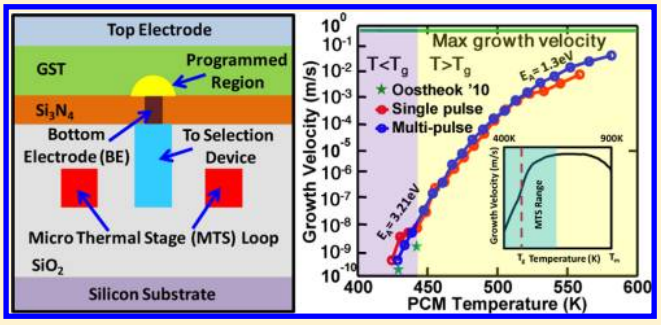

KEYWORDS: *Phase Change Memory, Crystallization, Fragility, Arrhenius Behavior, Growth Velocity, Nucleation, Nonvolatile*

Phase change memory (PCM) is considered as one of the most promising candidates for future nonvolatile memory technologies to meet the challenges facing the scaling limits of flash memory[1] and also to address the problem of the increasing performance gap between the main memory and the hard disk.[2] A number of high-capacity PCM chips have been demonstrated recently, showing the potential of PCM to be used in solid-state storage applications.[3,4] A continued effort is needed, however, to identify new phase change materials[5−7] and device structures that have low switching energy, higher speed, and better reliability. This requires fundamental understanding of the unconventional kinetics of the phase transition mechanism that determines the switching speed, retention, and multilevel programming of a PCM cell. Traditional methods of material characterization have involved using thin-film-based methods for measuring the key material properties such as crystallization temperature, crystallization time, and growth velocity.[7−11] Many of these works have been performed using static laser testing,[7] differential scanning calorimetry,[8] or sheet resistance measurements.[12] The results obtained from these measurements are representative of the phase change material under investigation but are not accurate enough to predict the reality of what happens in an actual PCM device. The issue is due to the limited range of operation (time and temperature) of these measurement techniques or unrealistic material and interface conditions involved. In this work, we have developed an experimental methodology that helps us accurately characterize different phase change materials to achieve results that are more technologically relevant.

First, we investigate the measurement of phase change material properties in the melt-quenched amorphous phase. Most of the previous material characterization experiments[10,13]

Received: March 12, 2014
Revised: April 28, 2014
Published: May 5, 2014

   dx.doi.org/10.1021/nl500940z | *Nano Lett.* 2014, 14, 3419−3426

are on the as-deposited amorphous phase of the phase change material whose retention properties are very different from that of the melt-quenched phase. It has been known that as-deposited amorphous films can have much longer crystallization times compared to the melt-quenched amorphous material.[11] This is mainly because in the latter case, no nucleation is required as the melt-quenched material typically is surrounded by crystalline material. Furthermore, the melt-quenched material also contains tiny crystal nuclei in the amorphous region that are formed during the quenching process that will act as initiating clusters for the crystallization process.[14,15] Neither of the above regions are typically found in an as-deposited amorphous film. Using the results from as-deposited phase can greatly overestimate the retention performance of the phase change material used in actual PCM devices. Hence, it is important to measure the material properties in the more technologically relevant melt-quenched phase.

One of the unique properties of the phase change materials that have made the nonvolatile memories possible is its ability to show fast crystallization (<100 ns) at the programming temperatures (>500 K) yet retain the amorphous memory state for over 10 years at low temperatures (typically 85 °C). This is possible because of the wide range of the growth velocity of phase change materials. In terms of the material properties, the growth velocity of the most common phase change material GST spans over 15 orders of magnitude for a temperature change of a few hundred degrees.[16] In addition, it was recently shown that the fragility of phase change materials like GST results in a lower activation energy for crystallization at higher temperatures ($T > T_g$, glass transition temperature), enabling the fast phase transformation properties.[8,17] Hence, it is important to do measurement of crystallization kinetics on short time scales and at higher temperatures to predict the application potential of phase-change materials with respect to ultrafast data storage. A number of recent works[9,10] have shown growth velocity measurements over wide range of temperatures, but all these measurements are based on blanket thin-films and use very sophisticated laser or calorimetry measurements. Although the thin-film and laser studies can yield results with a quick turn-around time, the crystallization kinetics can be different between a thin-film and in a practical PCM device. The physics of crystallization process is shown to be strongly dependent on the thickness of the phase change layer,[11] the size of the amorphous volume,[18] and interfaces involved.[19] With device scaling, the heterogeneous processes involving the interfaces with the neighboring oxide and electrode materials seem to dominate the crystallization speed.[20] Furthermore, the grain size of the active region has a significant role on the crystallization properties and also influences the stability and reliability of the intermediate resistance states for multilevel phase change memories.[16,20] It is hard to capture these effects in thin-film-based studies where mostly as-deposited amorphous material is used or in case of laser based melt-quenching[9,11] the size of the amorphous region is limited by the size and power of the laser spot (typically in micrometers, which is much larger than the PCM devices). In this work, we demonstrate the ability to characterize the phase change material properties at high speeds and using real PCM devices where all the effects of interfaces, grain size, thickness, and the melt-quench nature is captured.

The other key aspect of PCM device is its ability to show reliable switching properties even after several hundred million cycles. It is imperative that the phase change material achieves the required retention and switching speed until the target endurance limit. Most of the material characterization methods on thin films cannot capture how the material properties change after it has undergone repeated cycling. Studies have shown that cycling can cause material segregation in the phase change material and result in changes in the retention and switching properties.[21−23] However, there have not been any reports of how the material properties such as growth velocity and crystallization temperature change as a function of device cycling. In this work, we extract these key material properties as a function of device cycling. Knowledge of these key material properties is essential for developing a physical model for predicting the long-term reliability of PCM devices.

All of the above characterization requires an ultrafast heater that can control the local temperature of the phase change material independent from that of the electrical programming. For this purpose, we have developed a microthermal stage that is integrated with a vertical (mushroom) PCM cell along with an access transistor—typical of what one would find in a PCM memory array. Compared to our previous work of MTS for line-cells,[24,25] we have redesigned the MTS to ensure uniform temperature distribution throughout the phase change layer and also to reduce the thermal time constant below 1 μs. A unique feature of this design is that we have integrated MTS with a more practical and technologically relevant vertical PCM cell. We use this on-chip heater and thermometer to control the temperature at the programmed PCM cell to study the crystallization dynamics of phase change materials in the melt-quenched amorphous phase.

The top-view schematic of the microthermal stage and its integration with a phase change memory cell is shown in Figure 1a. The various device layers and the heater element are shown in the cross-sectional view of Figure 1b. The heater is designed in the form of a loop located below the phase change layer. The shape and location of the heating loop ensures uniform heating throughout the active programming region in the phase change layer. The heater has four terminals, namely I_+, I_-, V_+, and V_-, that enable us to accurately measure the heater resistance and also calibrate the temperature using a four-point method. The terminals I_+ and I_- branch into multiple lines to allow for minimum Joule heating at locations outside of the PCM cell. The V_+ and V_- lines allows for measuring the voltage drop ΔV_{MTS} across the active heating section of the MTS, $\Delta V_{MTS} = V_+ - V_-$. This voltage is much smaller than the actual voltage developed across the entire length of the heater terminals because of the additional interconnect resistance. Heat is generated in the narrow MTS loop area as current is passed through I_+ and I_- terminals and spreads to the PCM layer above. The silicon substrate below the heater acts as a major heat sink. In contrast to the previous design of MTS,[24,25] placing the heater below the PCM layer provides a more uniform temperature distribution throughout the phase change layer and also a reduced thermal time constant due to its location close to the heat sink (substrate). In comparison to the conventional thermal chuck, the thermal time constant of the MTS is several orders of magnitude smaller, as illustrated in Figure 1c. This enables the characterization of phase change memory devices on time scales that are relevant for actual device operation. The smaller time constant of MTS enables us to achieve higher heating rates of the order of 10^8 K/s that are close to that of the actual device heating rate of 10^{11} K/s. This fast heating rate can be used to directly probe into the rapid

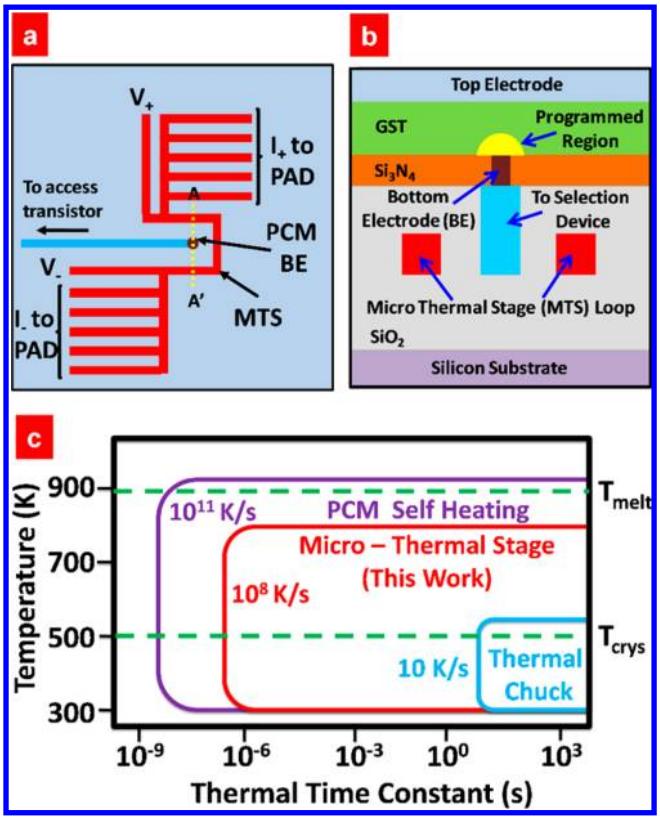

Figure 1. Microthermal stage. (a) Top view schematic of the microthermal stage (MTS) in the form of a loop surrounding the PCM cell. I_+, I_- and V_+, V_- are used for delivering current and measuring the heater voltage, respectively. The current terminals I_+ and I_- are narrow near the PCM device for maximum Joule heating and branch into multiple fingers away from the heating region to minimize the overall resistance. The PCM device is electrically programmed using a selection transistor.(b) Cross-sectional view (along AA′) showing the MTS heater located below PCM programming region. The MTS is made of tungsten and extends into the plane of the paper forming a loop just beneath PCM. (c) Comparison of thermal time constants for different methods of heating the phase change memory cell. MTS enables heating rates of up to 10^8 K/s, close to that of actual device programming conditions.

crystallization kinetics of phase change materials and obtain direct experimental measurement of crystallization parameters such as growth velocity and viscosity at temperatures far above the glass transition temperature.

The PCM device is programmed through an active transistor (or selection device) connected in series with the device. RESET programming is performed by passing a short, high-current pulse (typically 50 ns) directly through the PCM device while the transistor is turned ON (typically V_{gate} = 4.5 V). However, the SET programming or recrystallization can be achieved either by passing electrical current through the PCM device directly or by thermal heating using the MTS. The input to MTS can be either DC or pulse. (See Supporting Information Figure S1 for details on experimental setup.) Because the temperature at the MTS will be different from that at the PCM, detailed experimental characterization and modeling have been performed to precisely calibrate the PCM temperature and the thermal time constant.

Temperature calibration of MTS is performed using a thermal chuck; the extracted temperature coefficient (TCR) is 0.0017 K^{-1} and is then used to estimate the temperature at the MTS as a function of the input power (see Supporting Information Figure S2). Now, the temperature at the PCM layer is a fraction of the MTS temperature because of the thermal resistance contribution from the separating oxide and nitride layers (see Figure 1b). Because the device geometries are fixed, we can estimate this fraction using COMSOL simulations (see Supporting Information Figure S3a). The temperature rise in the PCM layer ($\Delta T_{PCM} = T_{PCM} - T_{AMB}$, where T_{AMB} is the ambient temperature, 300 K) is estimated to be 33% of that of the temperature rise in MTS ($\Delta T_{MTS} = T_{MTS} - T_{AMB}$) and is relatively uniform across the active device programming area. This temperature ratio is also found to be constant throughout the operating temperature range (see Supporting Information Figure S3b). The PCM temperature estimate was also corroborated by measuring the crystallization temperature (T_p) for the programmed PCM device and the temperature dependence of the crystalline PCM cell resistance (see Supporting Information Figure S4 and Figure S5). The thermal time constant due to the MTS at the PCM layer is measured to be 800 ns, reaching a temperature of 600 K (see Supporting Information Figure S6), which is close to the melting temperature (T_m) of many common phase change materials ($Ge_2Sb_2Te_5$ ~ 900 K, Sb_2Te_3 ~ 850 K, GeTe ~ 1000 K). The thermal time constant of the heater can be further improved by moving it closer to the heat sink (substrate) but at the expense of the power required to increase the heater temperature (see Supporting Information Figure S7). The MTS heater can withstand DC current densities of (J_{DC}) of 1.1 × 10^8 A/cm^2 that corresponds to temperatures over 1300 K. The temperature can be higher when short pulsed currents are used (see Supporting Information Figure S8). In terms of its cyclability the MTS can be continuously cycled over 10^6 cycles showing that MTS is a very robust platform to perform a number of different studies on the PCM device.

The electrical pulses applied to the MTS can be used to recrystallize the programmed amorphous region of the PCM devices. This recrystallization can be achieved by applying either a single large heating pulse or multiple small pulses. For the single pulse case, the current through the PCM device is monitored continuously by applying a constant electrical bias of 100 mV. The bias value is chosen to be small so as to avoid any Joule heating effects in the PCM device. The PCM current signal is in the range of several microamperes and needs to be amplified before observing it in the oscilloscope (see Supporting Information Figure S9). The MTS pulse is used to heat up the programmed amorphous volume and eventually recrystallize it to the low resistance state. Figure 2a shows the simultaneous measurement of the MTS pulse current (measured through I_- terminal) and the current through the PCM (amplified using *I*-to-*V* amplifier) as it undergoes phase transformation from the high resistance (low current) to low resistance (high current) state. Several things can be noted here. First, the crystallization process here happens under isothermal conditions as the PCM layer temperature has reached steady state in <1 μs. Under these conditions, the phase transformation happens along the amorphous crystalline boundary (marked by red arrows in Figure 2a inset) because the material is a growth-dominated phase change material.[18] We can observe that the PCM current increases rapidly after a certain time, at which point the amorphous−crystalline boundary starts to shrink smaller than the bottom electrode diameter. The phase transformation is complete when the PCM current reaches steady state, and the time taken to reach this

dx.doi.org/10.1021/nl500940z | Nano Lett. 2014, 14, 3419−3426

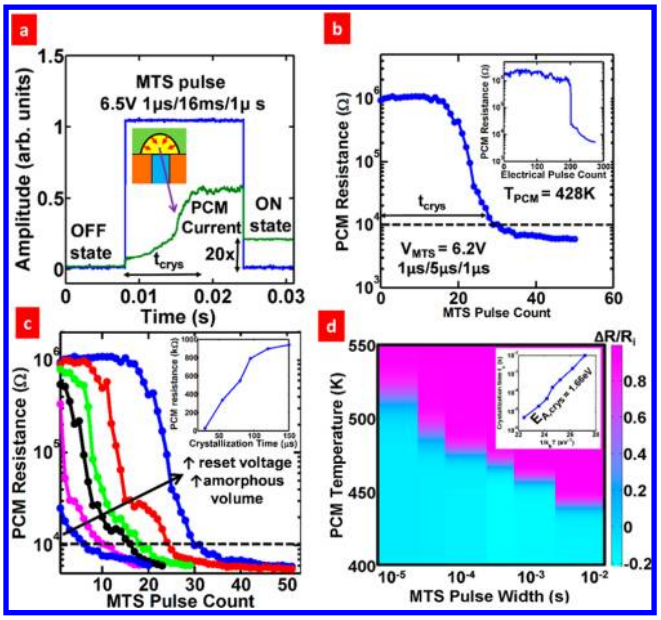

Figure 2. Crystallization of PCM device using microthermal stage. (a) Single pulse crystallization of PCM. The device is biased at 100 mV. The current through the PCM is amplified and monitored simultaneously as the MTS heating pulse is applied. The gradual increase in PCM current is due to the growth process happening in the amorphous region. The cell goes from 1 MΩ to 50 kΩ after applying the MTS pulse. (b) Multipulse PCM crystallization. The PCM device programmed in high resistance state is gradually recrystallized using identical thermal pulses of 5 μs width (T_{PCM} = 428 K < PCM crystallization temperature, T_p = 445 K). The inset shows the analogous crystallization of the PCM layer using a sequence of electrical SET pulses of 5 μs width (V_{SET} = 1.06 V < threshold voltage, V_{th}= 1.14 V). The resistance change is abrupt in electrical SET because of the filamentary nature of the crystalline region whereas the thermal pulses cause uniform gradual recrystallization from the amorphous−crystalline boundary. (c) Dependence of crystallization time (t_x) on the initial programmed resistance (amorphous fraction). An MTS pulse of 6.2 V, 5 μs (T_{PCM} = 428 K) is used to crystallize the PCM that is initially programmed with different reset voltages. The dotted line denotes a target resistance of 10 kΩ. The inset shows that the crystallization time (t_x) strongly depends on the amorphous fraction as the crystallization starts from the amorphous−crystalline boundary, typical of the growth-dominated materials. (d) time temperature transformation plot for isothermal heating of programmed PCM devices using MTS. The ratio of change in resistance to the initial resistance is plotted as a function of PCM temperature and MTS pulse width. This is similar to the static laser testing performed on thin films but is more relevant here as the material is in the melt-quenched amorphous phase. The inset shows the activation energy for crystallization calculated from the measured crystallization times.

steady state value can be considered as the crystallization time, t_{crys} as indicated in the figure. It is to be noted that this phase transformation is purely due to thermal effects. It can be seen that the PCM bias current measured after the application of MTS pulse is 20× higher compared to the case before the MTS pulse, indicating that the PCM device has been completely recrystallized. The PCM current is much higher during the heating phase because of the temperature-dependent electrical conductivity of phase change material[12] and drops after the MTS pulse is removed. Also, the sudden jump in the PCM current (at t = 8 ms) immediately following the application of the MTS pulse is attributed to the increased electrical conductivity of the amorphous phase at higher temperatures rather than the actual crystallization process, which happens at a later time (at t > 18 ms) while the MTS pulse is applied.

We can also bring about this phase transformation by applying a sequence of smaller but identical MTS thermal pulses to the PCM device because these pulses are additive in nature (see Supporting Information Figure S10). This multipulse scheme enables us to achieve partial recrystallization of the amorphous dome formed during RESET. Figure 2b shows a gradual decrease in the resistance for increasing number of identical heating pulses applied via MTS. This gradual recrystallization provides useful information for understanding a number of physical phenomena relating to the crystallization and switching dynamics of the phase change layer. By controlling the width and the amplitude of the heating pulse, we can determine a number of key parameters involving the nucleation and growth processes that take place during recrystallization. Furthermore, the gradual nature of recrystallization allows us to study the nature of partially programmed states. It is shown that the partial SET states tend to be different from that of their counterparts—the partial RESET states for the same given resistance value. This difference arises mainly because of the distribution of the partial filaments or crystalline nuclei regions inside the amorphous region.[26] Figure 2b inset shows the partial crystallization process using electrical SET pulses whose amplitude is below the electrical threshold voltage. The device switches to the ON resistance state after several pulses, and the transition is generally abrupt because it is hard to control the formation of these partial filaments using electrical SET. By using the MTS, it is possible to control the formation of these partial filaments gradually within the amorphous region and study the nature of these partially programmed states in greater detail, which is important in implementing multilevel memory for nonvolatile memory applications[27] and also in utilizing PCM as an electronic synapse for neuromorphic computing.[28] For the case of a multipulse scheme, we can define the crystallization time (t_{crys}) as the sum of the width of the pulses required to reach a minimum resistance value, in this case, 10 kΩ. The advantage of multipulse crystallization is that we can measure the crystallization times easily by just measuring the change in resistance at each pulse compared to the complicated current measurement involved in the single pulse method and is more practical for an on-chip measurement when the source terminal of the device cannot be accessed externally.

Another approach of obtaining intermediate resistance states is by doing partial RESET, where the volume of the amorphous region is controlled by applying relatively smaller amplitude RESET pulses. Hence, in this case the PCM device starts with a smaller amorphous volume or smaller resistance level. Figure 2c shows the recrystallization time as a function of the amorphous volume or cell resistance. It can be seen that the crystallization time (sum of the pulse widths required to reach a low resistance <10 kΩ) depends on the size of the amorphous volume. This is true in the case of growth-dominated materials where the crystallization generally starts from the amorphous−crystalline boundary.[18] In case of nucleation-dominated material such as GST, crystallization happens by the formation of small nuclei within the amorphous volume followed by the growth of certain supercritical nuclei that eventually merge to form a crystalline low resistance path. Because this nucleation process is generally homogeneous throughout the amorphous volume, the time taken for recrystallization does not strongly depend on the size of the amorphous volume.[18] However, with device

dx.doi.org/10.1021/nl500940z | Nano Lett. 2014, 14, 3419−3426

scaling, the interfaces start to play a major role in the nucleation process resulting in interface-driven heterogeneous nucleation and growth process.[20]

The short thermal time constant of the MTS allows for a very fast temperature rise in the phase change layer and enables isothermal annealing measurements similar to those of the static laser testing methods.[7] Figure 2d shows typical time temperature transformation (TTT) diagram[29] for a growth-dominated phase change material obtained by varying the pulse width and amplitude of the MTS pulses. It can be seen that complete phase transformation of the programmed amorphous state happens at 500 K for a MTS heating pulse of about 10 μs, resulting in heating rates >10^7 K/s. The activation energy for crystallization can be obtained from this plot and is found to be 1.66 eV for this phase change material. These TTT diagrams form a very important part of material characterization in identifying the retention capability of specific materials, and using the MTS, we can achieve accurate characterization of the phase change material in real programming conditions. Moreover, these measurements are performed on the melt-quenched phase of the material and are more technologically relevant than the as-deposited data typically reported using laser based methods.

Because crystallization is a thermally activated process, the time for crystallization exponentially depends on the temperature at the PCM layer and is a key parameter that determines the retention and switching properties of PCM. Figure 3a shows the multipulse crystallization of a fully programmed PCM device using MTS pulses of different amplitude

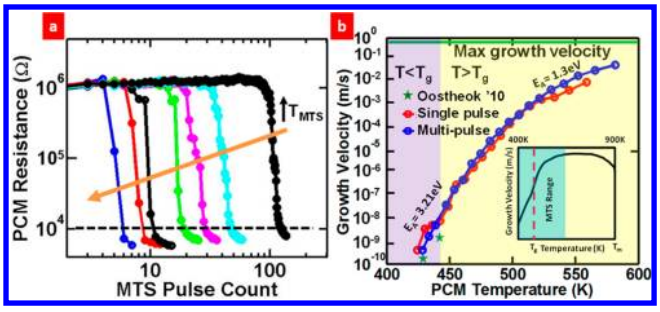

Figure 3. Extraction of crystal growth velocity. (a) Exponential dependence of PCM crystallization on temperature. MTS pulses of width 5 μs and different amplitudes (6.0–6.3 V, corresponding to T_{PCM} from 416–434 K) were used to crystallize the PCM device. All the PCM devices were initially reset to its fully amorphous state. The crystallization time can be extracted from the total number of MTS pulses required to reach the dotted resistance level (10 kΩ). (b) Dependence of crystal growth velocity on PCM temperature for a growth dominated phase change material. Growth velocity = [size of amorphous dome for a fully reset state (F ~ 70 nm)]/[total crystallization time]. F is the diameter of the bottom electrode. MTS allows direct measurement of growth velocity over 8 orders of magnitude (close to maximum growth velocity of 1 m/s) and temperatures well above the glass transition (T_g). Data are plotted for the growth velocity based on both the single pulse crystallization method (Figure 2a) and multipulse crystallization method (Figure 2b). The star denotes growth velocity data from Oostheok '10 obtained using TEM analysis[31] of fast growth phase change material thin films heated using thermal chuck. The inset shows the range of growth velocities and temperatures covered by MTS relative to the estimated values up to the melting temperature.[8] MTS allows us to extract the temperature dependence of growth velocity in the most useful and interesting regime (surrounding the T_g) of crystallization physics.

(temperature). By calculating the total number of pulses it takes to reach a low resistance of 10 kΩ, we can then extract the crystallization time as a function of the temperature at the PCM layer. The time for crystallization can also be extracted using the single pulse crystallization method (Figure 2a) by measuring the current through the PCM directly. Because the material used here is a growth dominated material, crystallization time can be considered as the time for the programmed amorphous region (domelike) to recrystallize along the amorphous–crystalline boundary. The height of amorphous volume (radii of the dome) can be approximated as the diameter of the bottom electrode, in this case 70 nm. (see Supporting Information Figure S11). We can then extract the growth velocity as a function of PCM temperature as shown in Figure 3b. For the first time, we have extracted the growth velocity data in real PCM devices, melt-quenched phase that spans 9 orders of magnitude (10^{-10} to 10^{-1} m/s) in the range of temperatures around the glass transition ($0.9T_g < T < 1.4T_g$). This is several orders faster than the typical range of data available from conventional calorimetry[30] or thermal chuck measurements[31] where measurements can generally be done only below the glass transition temperature and involve TEM analysis[31] of the samples after annealing at the desired temperature. Recently, growth velocity measurements at temperatures higher than T_g was reported on phase change materials AgInSbTe[9] and GeTe.[10] However, in both cases, the experiments were performed on thin films and using complicated laser based methods. The inset to Figure 3b shows the expected temperature dependence of growth velocity for a typical phase change material[10] up to the melting temperature, T_m. It can be seen that the growth velocity generally tapers as the temperature approaches T_m and the largest dynamic range of values lies around the glass transition temperature (T_g), which is covered by the MTS measurement range. The activation energy for crystallization is found to be maximum (3.2 eV) for temperatures around T_g and tapers off to about 1.3 eV at higher temperatures. This is because the temperature dependence of the atomic mobility (viscosity) is different at low temperatures where the material is a glass than at higher temperatures where it is a supercooled liquid.[8] If the temperature dependence at low temperatures were used to estimate the growth velocity at high temperatures (540 K), it leads to a gross overestimate of 2 m/s compared to the measured value of 10^{-2} m/s. It is this property that enables PCM to achieve both good retention (at $T < T_g$, higher E_A) and fast switching (for $T > T_g$, lower E_A). An experimental methodology of this sort, combined with appropriate crystal growth models, can provide a better understanding of crystallization physics in phase change materials and provide a path for systematically investigating the right choice of material for various new memory applications.

One of the key aspects of phase change memory is its good endurance where the cell can be repeatedly programmed for >10^8 cycles[1]. It has been reported[22,23,32] that repeated cycling of phase change materials can result in a gradual change in the device performance metrics such as reset current, device resistance, and switching time. This is attributed[23] to the material segregation that occurs in the programming region that results in a phase change material with different stoichiometric compositions over time. However, the exact nature of change in material properties have not been reported so far. The integration of MTS with a PCM device allows for us to study

dx.doi.org/10.1021/nl500940z | Nano Lett. 2014, 14, 3419–3426

the cycling dependence of material properties that are otherwise impossible using thin-film based measurements.

Using MTS, we characterize the crystallization growth velocity as a function of device cycling. Figure 4a shows the

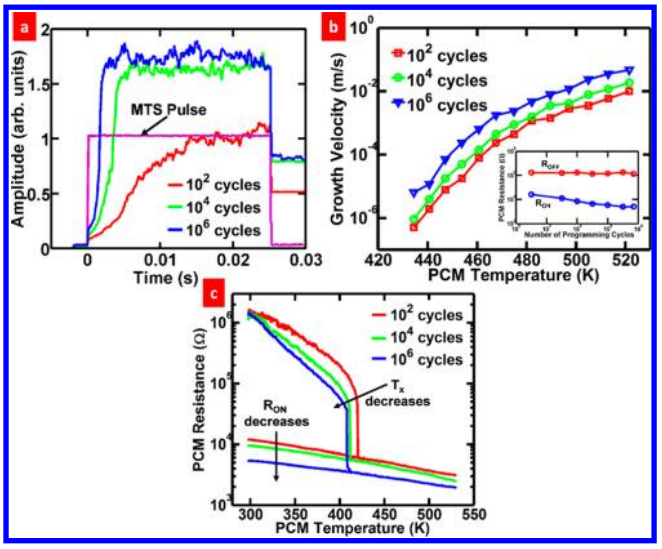

Figure 4. Effect of cycling on material properties. (a) Crystallization of programmed PCM device using MTS as a function of device cycling. An MTS pulse of 6 V (435 K) with a 25 ms width was used to heat the PCM device. The current through the PCM was also simultaneously observed in the oscilloscope by applying a PCM bias of 100 mV. The PCM device was subjected to continuous SET (1.2 V, 100 ns/1 μs/100 ns)/RESET (1.9 V, 10 ns/50 ns/10 ns) programming cycles before crystallizing with MTS. The crystallization time (t_x) is seen to decrease ($t_{x-10^6} < t_{x-10^4} < t_{x-10^2}$) with device cycling. (b) Growth velocity is extracted as a function of temperature for after different programming cycles. The inset shows the PCM SET/RESET resistance change as a function of device cycling. The growth velocity increases with device cycling due to the excess Sb content accumulated as a result of phase segregation. The activation energy however remains unaffected due to cycling. This has implications for the retention properties of cycled PCM devices. (c) Crystallization temperature (T_x) dependence on device cycling. A DC voltage sweep was applied to the MTS to crystallize the fully programmed PCM device. The crystallization temperature and the ON resistance decreases with device cycling.

MTS pulse (6 V, 25 ms) and simultaneous measurement of the crystallization current through the PCM device. The extracted growth velocity as a function of temperature for different programming cycles is shown in Figure 4b. It can be seen that for a given temperature, the growth velocity increases with the number of programming cycles, indicating that the crystallization process happens faster with device cycling. This can significantly impact the retention properties of cycled PCM devices. One possible explanation for this change in the crystallization property can be due to the accumulation of excess Sb content[33] in the programming region caused by phase separation as the device is subjected to huge thermal stress during the programming cycles. Furthermore, thin film studies[34] have shown that addition of excess Sb can greatly reduce the crystallization time, lower the crystallization temperature,[32] and also reduce the resistance in the crystalline state. These properties are attributed[34] to the rhombohedral structure of Sb-excess phase change materials that allow for fast crystallization. Figure 4c shows the crystallization of a fully programmed PCM device while ramping the PCM temperature using a DC voltage sweep at the MTS. It can be seen that the PCM crystallization temperature decreases with device cycling. Further, the Figure 4b inset and Figure 4c shows that the PCM SET resistance gradually decreases with increasing number of programming cycles due to the excess Sb content in the phase change material. This change in the crystallization properties with device cycling has to be considered while predicting the worst case retention and switching properties of PCM devices.

As observed from the previous growth velocity measurements, the activation energy for crystallization changes with temperature; in other words, crystallization is a non-Arrhenius process for phase change materials, especially for fast glass formers. However, the above methodology of directly measuring growth velocity using isothermal heating conditions can be applied only to growth-dominated phase change materials. In the case of nucleation-dominated materials such as $Ge_2Sb_2Te_5$, we can study the crystallization kinetics using nonisothermal conditions. In fact, during actual device programming, crystallization of PCM is a nonisothermal process, where the growth and nucleation dynamics change as a function of temperature. It has been reported earlier[12] that the crystallization temperature (T_p) of PCM increases with the heating rate and that the crystallization process is Arrhenius with constant activation energy. Using the MTS, we can achieve nonisothermal heating by applying various heating ramps to the PCM device. Figure 5a shows the experimental methodology

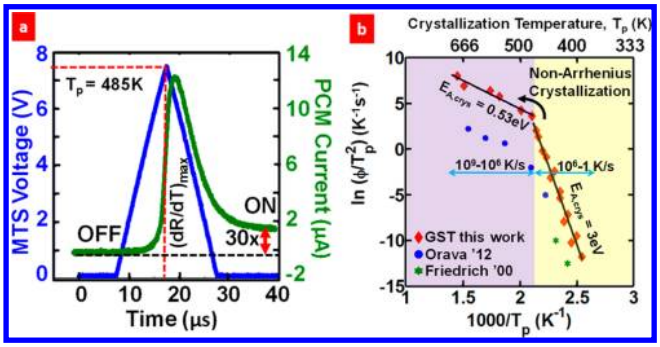

Figure 5. Non-Arrhenius crystallization. (a) Nonisothermal heating of PCM devices. A MTS heating pulse at a rate of 6×10^7 K/s is applied to a PCM cell in fully amorphous state. The current through the PCM device is monitored simultaneously by applying a small electrical bias of 0.1 V. The crystallization temperature (T_p) is measured where the change in PCM resistance (dR/dT) is a maximum. The overall change in PCM conductivity at the end of MTS heating is about 30× in this case. (b) Kissinger plot for nonisothermal heating of GST. Φ and T_p are the heating rate and the crystallization temperature. The slope of the plot gives the activation energy for crystallization $\ln(\Phi/T_p^2) = -E_{A,crys}/kT_p + c$. A non-Arrhenius behavior is observed at higher heating rates due to the fragile nature of GST. The results from thin-film studies (Orava '12[8] and Friedrich '00[12]) are also plotted for comparison.

used to extract the crystallization temperature T_p at different heating rates. The setup is similar to the single pulse crystallization method (see Supporting Information Figure S9), except that we use a triangular heating pulse rather than a square pulse. The PCM device is programmed in the fully RESET state. The current through the MTS and the PCM device are monitored simultaneously. The current through the PCM rapidly increases when the device undergoes crystallization, and the crystallization temperature T_p is given by the point where the change in PCM resistance is maximum. The

dx.doi.org/10.1021/nl500940z | Nano Lett. 2014, 14, 3419−3426

measured values of T_p at different heating rates are plotted in a special plot called a Kissinger plot,[35] shown in Figure 5b, which is used to study the properties of supercooled liquids such as glasses. The slope of the plot gives the activation energy of crystallization. For low temperatures, the measured activation energy is 3 eV, similar to that reported.[12] However, at higher heating rates (>10^6 K/s), the activation energy decreases to 0.53 eV, resulting in a non-Arrhenius behavior that is typically not captured by slow thermal chuck measurements. This behavior was attributed to the highly fragile nature of GST in its supercooled liquid state. The fragility occurs as a result of a sudden drop in the viscosity[8] of the phase change material for temperatures above the glass transition temperature. This lowering of viscosity at high temperatures allows for faster crystallization process as the atoms can now move much more freely in order to achieve the crystalline state in the material. The non-Arrhenius behavior of crystallization is thus crucial for enabling good data-retention at low temperatures (higher $E_{A,crys}$) and fast recrystallization at high temperatures (low $E_{A,crys}$). Recently, thin-film-based, fast calorimetric measurements[8] also revealed the fragile nature of GST; however, the results are for as-deposited films and require sophisticated experimental procedures. The difference in the measured values for the thin-film study[8] and our real PCM device is evident from Figure 5c, which arises due to the difference between the as-deposited and melt-quenched amorphous phase used in the respective experiments.

The key aspects of crystallization process such as growth velocity, non-Arrhenius behavior, and dependence on amorphous volume are investigated. The unique capabilities of the microthermal stage such as fast heating, high temperature, and the in situ nature enables experiments that provide valuable insights into the physical mechanisms of phase change that are otherwise impossible for traditional methods using blanket films, lasers, and thermal chuck. The capability to measure and characterize phase change materials in their melt-quenched phase, in practical device structures, at speeds and temperatures close to the device operating conditions, and as a function of device cycling provide an excellent wealth of experimental data not only to study the fundamental physics underlying the phase change mechanism but also to identify the right materials for the target applications.

■ ASSOCIATED CONTENT

Supporting Information

(1) Experimental setup.
(2) Temperature calibration of microthermal stage.
(3) Estimation of temparature at the PCM layer.
(4) Validation of PCM temperature estimate.
(5) Measurement of thermal time constant.
(6) Optimal design of MTS heater.
(7) Reliability of MTS heaters.
(8) Experimental setup—MTS single pulse crystallization.
(9) Additive nature of MTS pulses.
(10) Extraction of growth velocity.

This material is available free of charge via the Internet at http://pubs.acs.org.

■ AUTHOR INFORMATION

Corresponding Author

*R. Jeyasingh. E-mail: jrgdavid@stanford.edu. Mobile: +1 (408) 421-4943.

Present Address

¶100 Buckingham Drive, #202, Santa Clara, California 95051, United States.

Notes

The authors declare no competing financial interest.

■ ACKNOWLEDGMENTS

The authors would like to thank Intel Corporation for device fabrication and Der-Chang Kau (Intel) and Gianpaolo Spadini (Intel) for the valuable discussions. This work is supported by Intel through the Semiconductor Research Corporation (SRC) Global Research Collaboration (GRC) Customization Fund, the National Science Foundation (NSF, ECCS 0950305), and member companies of the Stanford Nonvolatile Memory Technology Initiative (NMTRI). National Science Foundation, ECS 0950305 Semiconductor Research Corporation, 2230.001

■ REFERENCES

(1) Wong, H.-S. P.; Raoux, S.; Kim, S.; Liang, J.; Reifenberg, J. P.; Rajendran, B.; Asheghi, M.; Goodson, K. E. Phase Change Memory. *Proc. IEEE* **2010**, *98*, 2201−2227.

(2) Burr, G. W.; Kurdi, B. N.; Scott, J. C.; Lam, C. H.; Gopalakrishnan, K.; Shenoy, R. S. Overview of Candidate Device Technologies for Storage-Class Memory. *IBM J. Res. Dev.* **2008**, *52*, 449−464.

(3) Lee, S. H.; Park, H. C.; Kim, M. S.; Kim, H. W.; Choi, M. R.; Lee, H. G.; Seo, J. W.; Kim, S. C.; Kim, S. G.; Hong, S. B.; et al.. Highly Productive PCRAM Technology Platform and Full Chip Operation: Based on $4F^2$ (84 nm Pitch) Cell Scheme for 1 Gb and beyond. In *2011 International Electron Devices Meeting*; IEEE: New Brunswick, NJ, 2011; pp 3.3.1−3.3.4.

(4) Kang, M. J.; Park, T. J.; Kwon, Y. W.; Ahn, D. H.; Kang, Y. S.; Jeong, H.; Ahn, S. J.; Song, Y. J.; Kim, B. C.; Nam, S. W.; et al.. PRAM Cell Technology and Characterization in 20 nm Node Size. In *2011 International Electron Devices Meeting*; IEEE: New Brunswick, NJ, 2011; pp 3.1.1−3.1.4.

(5) Simpson, R. E.; Fons, P.; Kolobov, A. V.; Fukaya, T.; Krbal, M.; Yagi, T.; Tominaga, J. Interfacial Phase-Change Memory. *Nat. Nanotechnol.* **2011**, *6*, 501−505.

(6) Takaura, N.; Ohyanagi, T.; Kitamura, M.; Tai, M.; Kinoshita, M.; Akita, K.; Morikawa, T.; Kato, S.; Araidai, M.; Kamiya, K.; et al. Charge Injection Super-Lattice Phase Change Memory for Low Power and High Density Storage Device Applications. *VLSI Technology Symp., 2013* **2013**, T130−T131.

(7) Cheng, H.-Y.; Raoux, S.; Jordan-Sweet, J. L. The Crystallization Behavior of Stoichiometric and off-Stoichiometric Ga−Sb−Te Materials for Phase-Change Memory. *Appl. Phys. Lett.* **2011**, *98*, 121911.

(8) Orava, J.; Greer, A. L.; Gholipour, B.; Hewak, D. W.; Smith, C. E. Characterization of Supercooled Liquid $Ge_2Sb_2Te_5$ and Its Crystallization by Ultrafast-Heating Calorimetry. *Nat. Mater.* **2012**, *11*, 279−283.

(9) Salinga, M.; Carria, E.; Kaldenbach, A.; Bornhöfft, M.; Benke, J.; Mayer, J.; Wuttig, M. Measurement of Crystal Growth Velocity in a Melt-Quenched Phase-Change Material. *Nat. Commun.* **2013**, *4*, 2371.

(10) Santala, M. K.; Reed, B. W.; Raoux, S.; Topuria, T.; LaGrange, T.; Campbell, G. H. Irreversible Reactions Studied with Nanosecond Transmission Electron Microscopy Movies: Laser Crystallization of Phase Change Materials. *Appl. Phys. Lett.* **2013**, *102*, 174105.

(11) Cheng, H.-Y.; Raoux, S.; Chen, Y.-C. The Impact of Film Thickness and Melt-Quenched Phase on the Phase Transition Characteristics of $Ge_2Sb_2Te_5$. *J. Appl. Phys.* **2010**, *107*, 074308.

(12) Friedrich, I.; Weidenhof, V.; Njoroge, W.; Franz, P.; Wuttig, M. Structural Transformations of $Ge_2Sb_2Te_5$ Films Studied by Electrical Resistance Measurements. *J. Appl. Phys.* **2000**, *87*, 4130.

(13) Weidenhof, V.; Friedrich, I.; Ziegler, S.; Wuttig, M. Laser Induced Crystallization of Amorphous $Ge_2Sb_2Te_5$ Films. *J. Appl. Phys.* **2001**, *89*, 3168.
(14) Lee, B.-S.; Burr, G. W.; Shelby, R. M.; Raoux, S.; Rettner, C. T.; Bogle, S. N.; Darmawikarta, K.; Bishop, S. G.; Abelson, J. R. Observation of the Role of Subcritical Nuclei in Crystallization of a Glassy Solid. *Science* **2009**, *326*, 980−984.
(15) Lee, B.-S.; Darmawikarta, K.; Raoux, S.; Shih, Y.-H.; Zhu, Y.; Bishop, S. G.; Abelson, J. R. Distribution of Nanoscale Nuclei in the Amorphous Dome of a Phase Change Random Access Memory. *Appl. Phys. Lett.* **2014**, *104*, 071907.
(16) Burr, G. W.; Tchoulfian, P.; Topuria, T.; Nyffeler, C.; Virwani, K.; Padilla, A.; Shelby, R. M.; Eskandari, M.; Jackson, B.; Lee, B.-S. Observation and Modeling of Polycrystalline Grain Formation in $Ge_2Sb_2Te_5$. *J. Appl. Phys.* **2012**, *111*, 104308.
(17) Ciocchini, N.; Cassinerio, M.; Fugazza, D.; Ielmini, D. Evidence for Non-Arrhenius Kinetics of Crystallization in Phase Change Memory Devices. *IEEE Trans. Electron Devices* **2013**, *60*, 3767−3774.
(18) Zhou, G.-F. Materials Aspects in Phase Change Optical Recording. *Mater. Sci. Eng., A* **2001**, *304*, 73−80.
(19) Cheng, H.-Y.; Raoux, S.; Munoz, B.; Jordan-Sweet, J. Influence of Interfaces on the Crystallization Characteristics of $Ge_2Sb_2Te_5$. In *2009 10th Annual Non-Volatile Memory Technology Symposium (NVMTS)*; IEEE: New Brunswick, NJ, 2009; pp 1−6.
(20) Wang, W.; Loke, D.; Shi, L.; Zhao, R.; Yang, H.; Law, L.-T.; Ng, L.-T.; Lim, K.-G.; Yeo, Y.-C.; Chong, T.-C.; et al. Enabling Universal Memory by Overcoming the Contradictory Speed and Stability Nature of Phase-Change Materials. *Sci. Rep.* **2012**, *2*, 360.
(21) Ryu, S. O.; Yoon, S. M.; Choi, K. J.; Lee, N. Y.; Park, Y. S.; Lee, S. Y.; Yu, B. G.; Park, J. B.; Shin, W. C. Crystallization Behavior and Physical Properties of Sb-Excess $Ge_2Sb_2Te_5$ Thin Films for Phase Change Memory (PCM) Devices. *J. Electrochem. Soc.* **2006**, *153*, G234.
(22) Boniardi, M.; Redaelli, A.; Ghetti, A.; Lacaita, A. L. Study of Cycling-Induced Parameter Variations in Phase Change Memory Cells. *IEEE Electron Device Lett.* **2013**, *34*, 882−884.
(23) Sarkar, J.; Gleixner, B. Evolution of Phase Change Memory Characteristics with Operating Cycles: Electrical Characterization and Physical Modeling. *Appl. Phys. Lett.* **2007**, *91*, 233506.
(24) Kim, S.; Lee, B.; Asheghi, M.; Hurkx, F.; Reifenberg, J. P.; Goodson, K. E.; Wong, H.-S. P. Resistance and Threshold Switching Voltage Drift Behavior in Phase-Change Memory and Their Temperature Dependence at Microsecond Time Scales Studied Using a Micro-Thermal Stage. *IEEE Trans. Electron Devices* **2011**, *58*, 584−592.
(25) Ahn, C.; Lee, B.; Jeyasingh, R. G. D.; Asheghi, M.; Hurkx, G. A. M.; Goodson, K. E.; Philip Wong, H.-S. Crystallization Properties and Their Drift Dependence in Phase-Change Memory Studied with a Micro-Thermal Stage. *J. Appl. Phys.* **2011**, *110*, 114520.
(26) Mantegazza, D.; Ielmini, D.; Pirovano, A.; Lacaita, A. L. Incomplete Filament Crystallization During Set Operation in PCM Cells. *IEEE Electron Device Lett.* **2010**, *31*, 341−343.
(27) Nirschl, T.; Philipp, J. B.; Happ, T. D.; Burr, G. W.; Rajendran, B.; Lee, M.-H.; Schrott, A.; Yang, M.; Breitwisch, M.; Chen, C.-F.; et al.. Write Strategies for 2 and 4-Bit Multi-Level Phase-Change Memory. In *Int. Electron Devices Meet., 2007*; IEEE: New Brunswick, NJ, 2007; pp 461−464.
(28) Kuzum, D.; Jeyasingh, R. G. D.; Lee, B.; Wong, H.-S. P. Nanoelectronic Programmable Synapses Based on Phase Change Materials for Brain-Inspired Computing. *Nano Lett.* **2012**, *12*, 2179−2186.
(29) Wuttig, M.; Yamada, N. Phase-Change Materials for Rewriteable Data Storage. *Nat. Mater.* **2007**, *6*, 824−832.
(30) Kalb, J. A.; Wen, C. Y.; Spaepen, F.; Dieker, H.; Wuttig, M. Crystal Morphology and Nucleation in Thin Films of Amorphous Te Alloys Used for Phase Change Recording. *J. Appl. Phys.* **2005**, *98*, 054902.
(31) Oosthoek, J. L. M.; Kooi, B. J.; De Hosson, J. T. M.; Wolters, R. A. M.; Gravesteijn, D. J.; Attenborough, K. Growth Rate Determination through Automated TEM Image Analysis: Crystallization Studies of Doped SbTe Phase-Change Thin Films. *Microsc. Microanal.* **2010**, *16*, 291−299.
(32) Oosthoek, J. L. M.; Attenborough, K.; Hurkx, G. A. M.; Jedema, F. J.; Gravesteijn, D. J.; Kooi, B. J. Evolution of Cell Resistance, Threshold Voltage and Crystallization Temperature during Cycling of Line-Cell Phase-Change Random Access Memory. *J. Appl. Phys.* **2011**, *110*, 024505.
(33) Nam, S.-W.; Kim, C.; Kwon, M.-H.; Lee, H.-S.; Wi, J.-S.; Lee, D.; Lee, T.-Y.; Khang, Y.; Kim, K.-B. Phase Separation Behavior of $Ge_2Sb_2Te_5$ Line Structure during Electrical Stress Biasing. *Appl. Phys. Lett.* **2008**, *92*, 111913.
(34) Cheng, H.-Y. C.; Raoux, S.; Kim, S. K.; BrightSky, M.; Cheek, R.; Lung, H.-L.; Lam, C. The Crystallization Behavior of Ge-Sb-Te Materials as a Function of Composition for Phase-Change Memory. *Eur. Phase Change Ovonic Symp.* **2013**, S3−03.
(35) Kissinger, H. E. Reaction Kinetics in Differential Thermal Analysis. *Anal. Chem.* **1957**, *29*, 1702−1706.